Aust. J. Phys., 1985, **38**, 507–18

Extinction in Polycrystalline Materials*

T. M. Sabine

School of Physics and Materials, N.S.W. Institute of Technology,
P.O. Box 123, Broadway, N.S.W. 2007.

Abstract

An expression is given for an extinction factor appropriate to powders composed of spherical perfect crystal grains or subgrains. This factor extrapolates to the dynamical theory value for the plane parallel plate in the symmetric Bragg case. Experimental tests of the theory have been made by neutron diffraction experiments on polycrystalline specimens of MgO of controlled grain size. Agreement is excellent to an extinction level of $y = 0{\cdot}60$.

1. Introduction

The Rietveld (1969) method has become widely used as a procedure for extracting crystallographic information from powder data. In its original form only the intensities of the Bragg peaks were used; however, Sabine and Clarke (1977) and Sabine (1980) extended it to include diffuse scattering. In the Rietveld method the quantity

$$M = \sum_i w_i (y_i^{\text{obs}} - y_i^{\text{calc}})^2$$

is minimized, where y_i^{obs} is the number of neutrons scattered into the ith time or angle channel and y_i^{calc} is the number of neutrons which would have been scattered into this channel if the assumed model of the target and of the resolution function of the instrument is correct. The weight w_i of the ith observation is the reciprocal of the variance of y_i^{obs}. The assumption that this minimization leads to the best estimate of the least squares parameters depends critically on the physical reality of the model from which the calculated ordinate is derived. One important component of the model is extinction.

Extinction is customarily classified as primary or secondary. Primary extinction is the reduction in intensity of the Bragg reflected beam by re-scattering into the direction of the incident beam as it passes through successive planes in a perfect crystal. Secondary extinction results from the presence in the crystal of mosaic blocks of identical orientation. The Bragg reflected beam from one mosaic block will be depleted by scattering into the primary beam direction by a block of the

* Dedicated to Dr A. McL. Mathieson on the occasion of his 65th birthday.

0004-9506/85/030507$02.00

same orientation. Primary extinction is proportional to the size of the perfect crystal block, while secondary extinction is proportional to the closeness in orientation of the successive blocks.

When extinction phenomena are operating, the integrated intensity of the diffracted beam is less than that calculated from the kinematic approximation. This intensity loss is balanced by an increase in the intensity of the transmitted beam.

In a polycrystalline material, in which all orientations of mosaic blocks are present with equal probability, secondary extinction, in the sense used in single crystal diffraction experiments, has no meaning. It is replaced by multiple scattering in which the diffracted beams act as incident beams for the generation of further Debye–Scherrer cones. This process augments the diffuse scattering, rather than the primary beam, at the expense of the diffracted beam. In this paper the term extinction will be used to refer to primary extinction.

Cassels (1950) drew attention to the observation by Whitaker and Bayer (1939) that polycrystalline materials were more transparent to neutrons when the microcrystals were large. He concluded that the scattering was being modified by extinction effects and suggested that the grain size in a polycrystal should not be greater than 0·5 μm. Fermi *et al.* (1947), in a study of the transmission of slow neutrons through microcrystalline material, concluded that an appreciable reduction in the intensity of Bragg peaks because of extinction would not occur for crystals of linear dimensions smaller than 1 μm. Ekstein (1951) treated the problem of neutron scattering by a perfect spherical crystal in the second Born approximation and showed that, for a typical scatterer, the correction to the kinematical result was 9% for a particle diameter of 10 μm. Sabine and Dawson (1963), during a study of the ionic state of beryllium oxide, showed experimentally that severe extinction effects were present in powder diffraction data, obtained from polycrystalline specimens with a grain size greater than 20 μm at a neutron wavelength of 1 Å.

In many cases the size of the perfect microcrystals will be smaller than the grain size or particle size in a powder specimen because of the presence of a subgrain structure. However, for brittle materials it is likely that each grain is a perfect crystal and extinction is the major mechanism for departure from kinematic scattering.

2. Theory

Notation

Crystallographic notation will be used in this work. The incident wavevector is $\boldsymbol{k}_i$ and the diffracted wavevector is $\boldsymbol{k}_f$. For elastic scattering the magnitude of both these vectors is $1/\lambda$, where λ is the neutron wavelength. The scattering vector is denoted by $\boldsymbol{k} = \boldsymbol{k}_f - \boldsymbol{k}_i$, $k = 2\sin\theta/\lambda$, while $\boldsymbol{k}_B$ is the scattering vector corresponding to the exact Bragg condition; θ is half the angle between $\boldsymbol{k}_i$ and $\boldsymbol{k}_f$.

Energy Transfer Equations

It is assumed that the powder consists of a random distribution of spherical particles, and extinction takes place within each particle. True absorption within a particle will be taken as negligible. The observed intensity will be the intensity of scattering at the exit surface of each particle summed over the number of particles oriented to satisfy the Bragg condition. There is no coherence in the scattering from different particles.

Following Zachariasen (1945, 1967) and Hamilton (1957), the Darwin energy transfer equations are used:

$$\partial I_i/\partial t_i = -\sigma I_i + \sigma I_f, \tag{1}$$

$$\partial I_f/\partial t_f = -\sigma I_f + \sigma I_i, \tag{2}$$

where I_i is the intensity of the beam along t_i, which is parallel to the incident beam, while I_f is the intensity along t_f, which is in the direction of the diffracted beam. The coupling constant σ is the cross section per unit volume for Bragg scattering into an elementary region of reciprocal space close to k_B.

Exact solutions of equations (1) and (2) can be found only for the infinite plane parallel plate of thickness D_0 in (i) the symmetric Laue case, in which the diffracted beam leaves the plate on the opposite side to the entry point of the incident beam and both beams make the same angle with the plate normal; (ii) the symmetric Bragg case, in which the diffracted beam exits from the same side as the incident beam enters. Again both make the same angle with the plate normal.

The solutions for the intensity at the exit surface of the crystal are, respectively, for the Laue and Bragg cases

$$I_f = I_i^0\{1-\exp(-2\sigma D)\}, \qquad D = D_0/\cos\theta; \tag{3a, b}$$

$$I_f = I_i^0\,\sigma D/(1+\sigma D), \qquad D = D_0/\sin\theta. \tag{4a, b}$$

Here D is the average pathlength of the diffracted beam in the crystal and I_i^0 is the intensity of the beam entering the crystal. The intensity of the diffracted beam at the exit surface under kinematic conditions is, in both cases,

$$I_f^{kin} = I_i^0\,\sigma D. \tag{5}$$

Evaluation of σ

To find an expression for the extinction coefficient, it is first necessary to express σ in terms of crystallographic quantities. The starting point is the kinematic differential cross section for coherent elastic scattering from a crystal without defects, given by

$$\left(\frac{d\sigma}{d\Omega}\right)_{coh} = |F|^2 \left|\sum_{j=0}^{N-1} \exp(2\pi i\, k \cdot r_j)\right|^2, \tag{6}$$

where F is the structure factor per unit cell and contains the Debye–Waller factor, N is the number of unit cells in the crystal and r_j is the position vector of the origin of the jth unit cell. After introduction of the delta function and integration over $d\Omega$ (Marshall and Lovesey 1971), the cross section per unit volume for a single Bragg reflection k_B is given by

$$\sigma(k) = (N_c^2 \lambda^2 F^2/\sin\theta)\delta(k_B - k) \tag{7a}$$

or

$$\sigma(\Delta k) = Q_k\,\delta(\Delta k). \tag{7b}$$

Here $Q_k V$ is the kinematic integrated intensity of the reflection on the k scale, V is the volume of the crystal and N_c is the number of unit cells per unit volume.

For a crystal of finite size a profile must be chosen for $\delta(\Delta k)$. Zachariasen (1967) and Becker and Coppens (1974) used Fresnellian functions, whereas Hamilton (1957) used a rectanguar function. Since the dynamical theory predicts definite reflection profiles it is likely that the function chosen for $\sigma(\Delta k)$ will have a strong influence on the final result. This proves to be the case. The possible profiles are

$$\begin{aligned}
\sigma(\Delta k) &= Q_k T/\{1+(\pi T\Delta k)^2\} && \text{Lorentzian (L);}\\
&= Q_k T \sin^2 \pi T\Delta k/(\pi T\Delta k)^2 && \text{Fresnellian (F);}\\
&= Q_k T \exp\{-\pi(T\Delta k)^2\} && \text{Gaussian (G);}\\
&= Q_k T, \quad |\Delta k| \leqslant 1/2T\\
&= 0 \quad \text{otherwise} && \text{Rectangular (R);}\\
&= Q_k T(1-|\Delta k|T), \quad |\Delta k| \leqslant 1/T\\
&= 0 \quad \text{otherwise} && \text{Triangular (T).}
\end{aligned}$$

For each profile, conversion to the 2θ scale and calculation of the integral breadth leads to the Scherrer equation with T the volume average of the thickness of the crystal normal to the diffracting plane (Wilson 1949).

3. Calculation of the Extinction Coefficient

The extinction coefficient y is defined as the ratio of the integrated intensity of the reflection to the integrated intensity it would have under kinematic conditions. Then, for the Laue case from equations (3) and (5), we have

$$y = \tfrac{1}{2} \int [1-\exp\{-2\sigma(\Delta k)D\}]\, \mathrm{d}(\Delta k) \Big/ \int \sigma(\Delta k) D\, \mathrm{d}(\Delta k),$$

and for the Bragg case from equations (4) and (5)

$$y = \int \frac{\sigma(\Delta k)\, \mathrm{d}(\Delta k)}{1+\sigma(\Delta k)D} \Big/ \int \sigma(\Delta k)\, \mathrm{d}(\Delta k).$$

The limits of integration depend on the specific form of $\sigma(\Delta k)$. Substitution of each expression for $\sigma(\Delta k)$ into these equations and integration over Δk leads to the following expressions for y. We note first that the only non-trivial integrations are [see, respectively, Michell and Belz (1950) and Whittaker and Watson (1952)]

$$\int \frac{\mathrm{d}t}{(1+t^2)^n}, \qquad \int_0^\infty \frac{\sin^n mt}{t^n}\,\mathrm{d}t, \tag{8a, b}$$

and we write $x = Q_k DT$. The extinction coefficients for the two cases are

Laue:
$$y_L = 1 - \frac{x}{2} + \frac{x^2}{4} - \frac{5x^3}{48} + \ldots,$$
$$y_F = 1 - \frac{2x}{3} + \frac{11x^2}{30} - \frac{151x^3}{945} + \ldots,$$
$$y_G = 1 - \frac{2x}{2!\,2^{\frac{1}{2}}} + \frac{4x^2}{3!\,3^{\frac{1}{2}}} - \frac{8x^3}{4!\,4^{\frac{1}{2}}} + \ldots,$$
$$y_R = (1/2x)\{1 - \exp(-2x)\},$$
$$y_T = \frac{1}{x}\left(1 - \frac{1}{2x}\{1 - \exp(-2x)\}\right);$$

Bragg:
$$y_L = 1/(1+x)^{\frac{1}{2}},$$
$$y_F = 1 - \frac{2x}{3} + \frac{11x^2}{20} - \frac{151x^3}{315} + \ldots,$$
$$y_G = 1 - \frac{x}{2^{\frac{1}{2}}} + \frac{x^2}{3^{\frac{1}{2}}} - \frac{x^3}{4^{\frac{1}{2}}} + \ldots,$$
$$y_R = 1/(1+x),$$
$$y_T = (2/x^2)(x - \ln|1+x|).$$

When profile analysis is being used, the necessity for an integration over Δk may be questioned. Each profile point is the result of an integration over one step in the scan. The size of each step in either angle or time is very much greater than the width of a reflection from a perfect crystal. The intensity measured at each profile point is therefore the integrated intensity of the perfect crystal reflection.

4. Comparison with Dynamical Theory

The exact solution for the infinite parallel plate in the symmetric Bragg case is (Zachariasen 1945)

$$y = (\tanh A)/A, \tag{9}$$

where $A = N_c \lambda F D_0/\sin\theta$, and where F is the structure factor magnitude per unit cell, which includes the Debye–Waller factor. The substitutions $Q_k = N_c^2\lambda^2/F^2 \sin\theta$, $D = D_0/\sin\theta$, $T = D_0$ in equation (8) show that A is equal to $x^{\frac{1}{2}}$. For thick crystals the expression for y extrapolates to $y = x^{-\frac{1}{2}}$.

For the Laue case Zachariasen (1945) gave

$$y = \sum_{n=0}^{\infty} \mathrm{J}_{2n+1}(2A)/A,$$

where $A = N_c \lambda F D_0 / \cos\theta$ and $\mathrm{J}_{2n+1}(2A)$ is a Bessel function. The substitutions $D = D_0/\cos\theta$ and $T = D_0 \tan\theta$ (which were also used by Zachariasen) give $A = x^{\frac{1}{2}}$, and the asymptotic expression is $y = 1/2x^{\frac{1}{2}}$.

For the expressions found in Section 3 the extrapolations are

$$y_L^B = x^{-\frac{1}{2}}, \qquad y_L^L = 1/1{\cdot}25x^{\frac{1}{2}}.$$

The statement by Becker and Coppens (1974) that the transfer equations incorrectly describe the extinction effect in an infinite parallel plate is not substantiated in the Bragg case for a Lorentzian profile.

5. Application to Sphere

It is assumed here that the Bragg case is appropriate to extinction in a spherical crystal, an assumption also made by Zachariasen (1945). Because of extrapolation of the flat plate case to the dynamical theory result a Lorentzian profile is used. Wilkins (1980) in a detailed study of dynamical diffraction from imperfect crystals showed that the dynamical theory expression (9) is a much better approximation to primary extinction in a block of side l_0, if the plate thickness parameter is taken as $l_0 \sin\theta$.

Use of this result for the sphere (with $T = \frac{3}{2}r$ and $D = \frac{3}{2}r \sin\theta$, where r is the radius of the sphere) leads to

$$x = \tfrac{9}{4} N_c^2 \lambda^2 F^2 r^2. \tag{10}$$

Ekstein (1951) found that

$$y = 1 - \tfrac{7}{4} F^2 N_c^2 \lambda^2 r^2.$$

If this is taken as part of a series expansion, the present result is

$$y = 1 - \tfrac{9}{8} F^2 N_c^2 \lambda^2 r^2.$$

In comparison Becker and Coppens (1974) obtained for the sphere

$$y = 1 - \tfrac{99}{70} F^2 N_c^2 \lambda^2 r^2.$$

6. Experimental Test of the Extinction Formula

Experiment

The material chosen for an experimental study of the extinction formula was magnesium oxide. The crystal data is given by (Howard and Sabine 1974)

Space group $O_h^5 - Fm3m$ (no. 225);

$$\epsilon = 3{\cdot}65; \qquad Z = 4;$$

$$\text{Mg} = 4(a): \ 0,0,0; \qquad \text{O} = 4(b): \ \tfrac{1}{2},\tfrac{1}{2},\tfrac{1}{2};$$

$$a = 4{\cdot}21145 \pm 0{\cdot}000025 \text{ Å}.$$

The only variable structural parameters are the thermal vibration parameters for each atom. These have been studied extensively and are the subject of a review by Barron (1977), who concluded that the best value of the overall temperature factor for even index Bragg peaks measured by neutron diffraction is $0{\cdot}314 \pm 0{\cdot}010$ Å^2.

In the context of the present work, it is interesting to note that two results higher than this have been obtained by Beg (1976), using elastic neutron powder diffraction on a sample whose grain size was estimated by Barron (1977) to be 3 μm, and by Sanger (1969), who used neutron irradiation to destroy the perfection of a single crystal. Their results were $0{\cdot}354 \pm 0{\cdot}008$ Å^2 (Beg 1976) and $0{\cdot}343 \pm 0{\cdot}014$ Å^2 (Sanger 1969).

In the present work specimens of polycrystalline MgO were prepared by cold pressing and sintering or, for specimen 20M, by hot pressing. The grain growth was controlled by varying the time and temperature for sintering.

Table 1. Integrated intensity per gram for Bragg reflections from specimens of different grain size

Parameter B is the overall temperature factor from a Rietveld analysis. Integrated intensities are given in neutron counts per gram, with errors in parentheses

Specimen	Mass (gm)	D (μm)	$I(200)$	$I(400)$	$I(600,442)$	B
2M	6·756	0·7	13950(50)	3724(30)	9384(50)	0·366(0·007)
4M	6·679	2·0	14106(50)	3549(30)	9342(50)	0·337(0·007)
20M	10·58	14·0	9395(35)	2577(25)	6880(40)	0·246(0·007)
50M	16·77	20·0	7689(40)	2119(30)	5934(40)	0·179(0·006)
50M′	8·78	20·0	8104(30)	2289(40)		

Each specimen was a cylinder approximately 1 cm diameter by 2 cm high. The masses are shown in Table 1. Specimen 50M′ is approximately half the mass of specimen 50M. This additional pattern was taken as a check on the homogeneity of the neutron beam.

A scanning electron microscope was used to determine the grain size distribution; typical micrographs are shown in Fig. 1. In all cases, several micrographs were obtained from different parts of the specimen and measured by hand to find the distribution of grain diameters. The corresponding distributions are shown in Fig. 2.

Neutron diffraction data was collected on a conventional neutron powder diffractometer (with monochromator take-off angle of 30°) on the reactor HIFAR. The configuration of the instrument was unchanged during the course of the experiment. The neutron wavelength was 1·088 Å and the range of scattering angle was 15–120° of 2θ. True absorption is negligible in MgO specimens of this size. Multiple scattering, which weakens the Bragg peaks and augments the diffuse scattering, will have an approximately equal effect in each specimen. It should be noted that the absolute effect of multiple scattering is not small. The intensity of each Bragg peak is reduced by approximately 10% from the kinematic value.

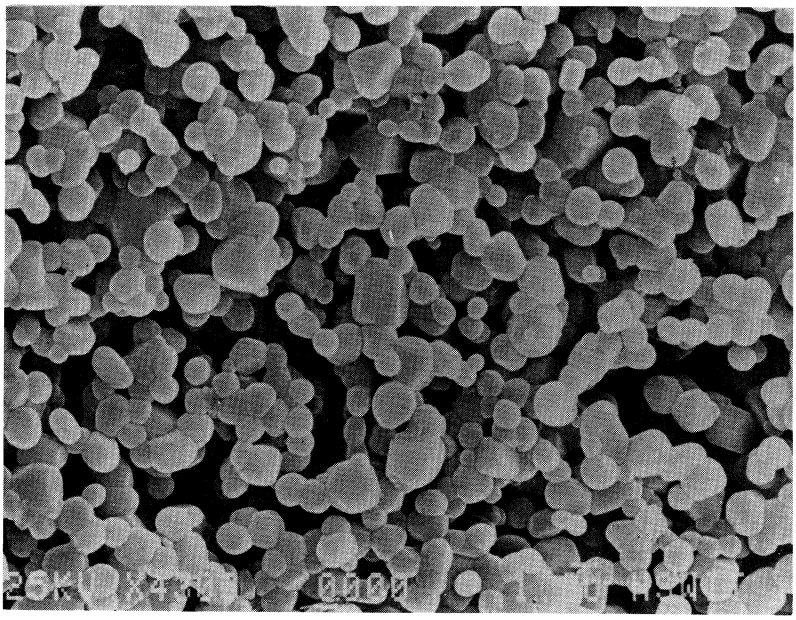

(*a*)

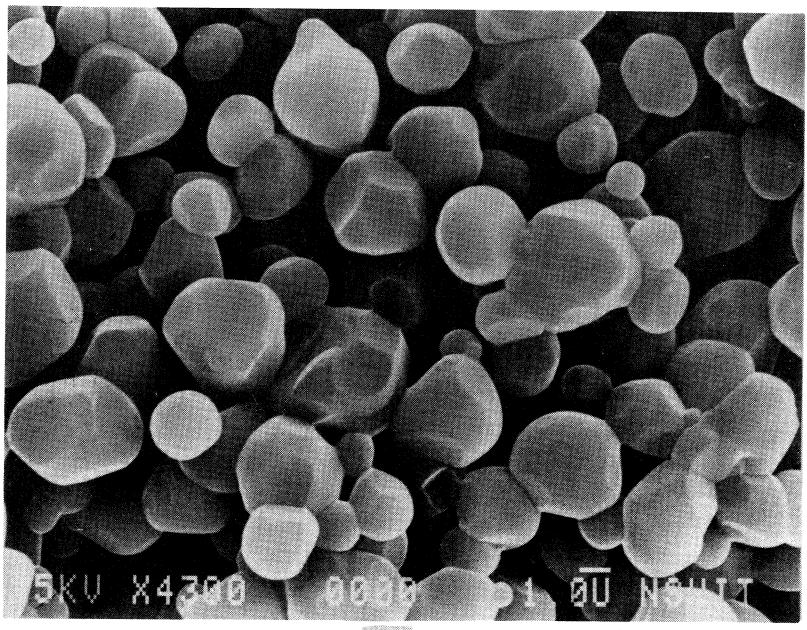

(*b*)

Fig. 1. Electron micrographs of the four specimens of MgO: (*a*) 2M (× 4300); (*b*) 4M (× 4300); (*c*) 20M (× 2200); (*d*) 50M (× 540). The magnifications are approximately 15% larger than the actual magnifications, which were determined from the calibration marks on the films and used in the calculations of extinction coefficients.

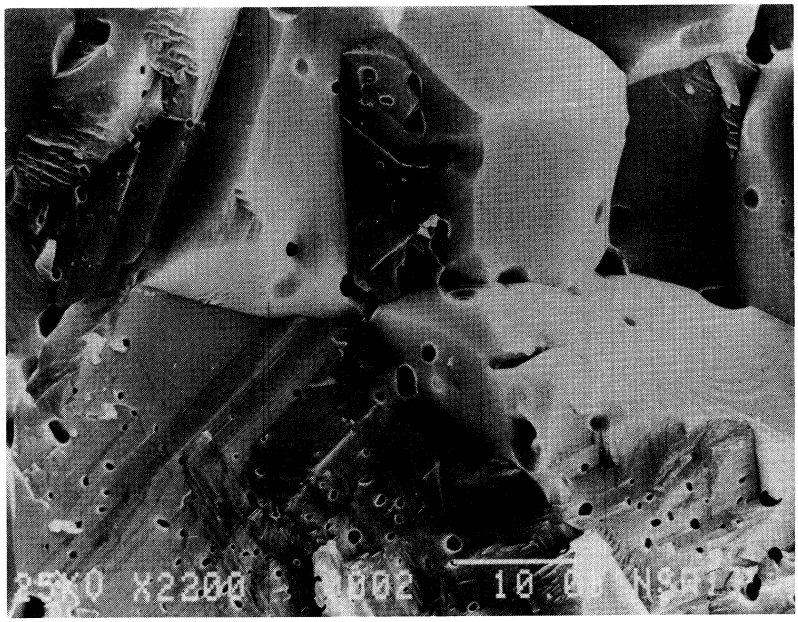

(*c*)

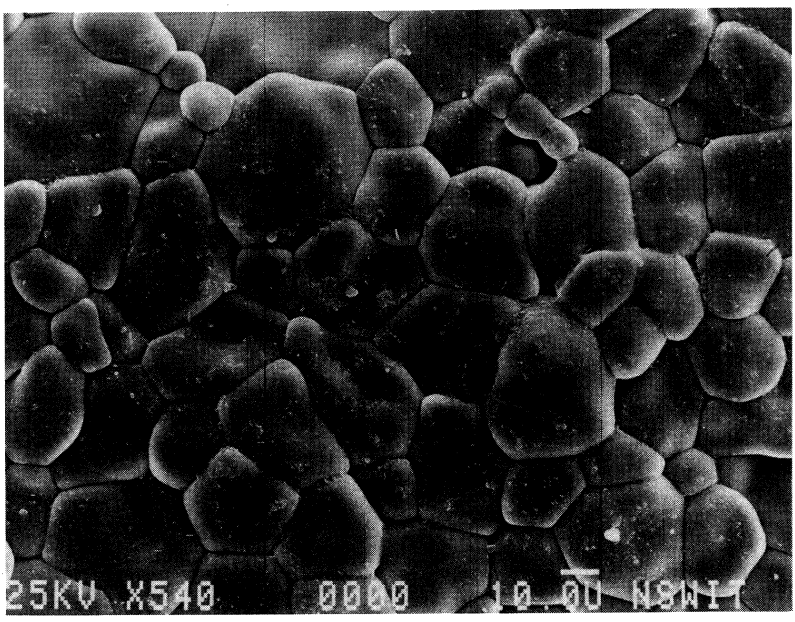

(*d*)

Figs 1*c* and 1*d* [*see opposite*].

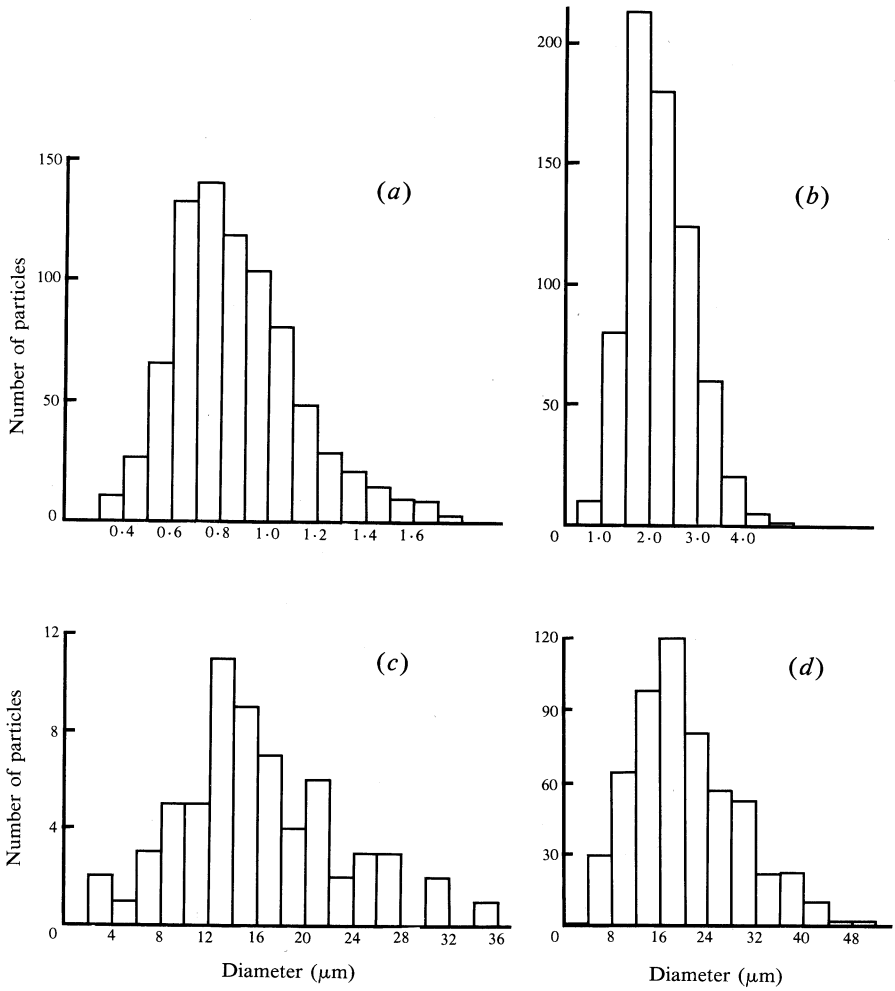

Fig. 2. Grain size distributions in four specimens of MgO: (*a*) 2M (25 hours at 1300 °C, 614 data points); (*b*) 4M (50 hours at 1300 °C, 802 data points); (*c*) 20M (hot pressed at Lucas Heights, 64 data points); and (*d*) 50M (12 days at 1450 °C, 549 data points).

Analysis of Results

The integrated intensity of the (200), (400) and (600, 442) reflections was measured by summing the ordinates of the profile. The background was measured on either side of the peak and extrapolated to the region under the peak. The results of these measurements are shown in Table 1. The temperature factors were determined by Rietveld analyses of each set of data. The program used (Hewat 1974) had no provision for refinement of an extinction parameter. For each set of data the background was estimated graphically and the variables in the least squares analysis were the scale factor, average isotropic temperature factor, the lattice parameter, zero point and profile parameters.

The values of the overall temperature factor B are also given in Table 1 and show a strong dependence on grain size. The trend towards lower values of B for larger grains is consistent with the operation of extinction effects. E. Prince (personal communication) obtained a powder pattern from specimen 20M with a neutron wavelength of 1·54 Å and derived the value $B = 0{\cdot}04 \pm 0{\cdot}03$.

7. Extinction Parameters

The histograms of grain size distribution shown in Fig. 2 express the frequency of occurrence f_i of a grain diameter D_i. To obtain the extinction parameter for the specimen the extinction parameter for each grain size D_i is multiplied by the volume fraction of the specimen composed of grain size D_i, and the result summed over i:

$$y = \left(\sum_i f_i D_i^3\right)^{-1} \sum_i f_i D_i^3 (1+x_i)^{-\frac{1}{2}}.$$

The y_{th} values given in Table 2 were calculated from this expression using equation (10) to give x_i. A temperature factor of 0·34 was assumed.

To determine the experimental extinction parameters, the assumption was made that the data for specimen 2M and 4M were extinction free. Then, y_{exp} is the ratio of the integrated intensities per gram for 20M and 50M to the mean value for 2M and 4M.

Table 2. Calculated and measured values of the extinction parameter for specimens of different grain size

Specimen	200		400		600	
	y_{exp}	y_{th}	y_{exp}	y_{th}	y_{exp}	y_{th}
2M	1·0	1·0	1·0	1·0	1·0	1·0
4M	1·0	0·99	1·0	0·99	1·0	0·99
20M	0·67	0·676	0·71	0·695	0·73	0·724
50M	0·55	0·593	0·58	0·612	0·63	0·643
50M′	0·58	0·593	0·63	0·612		

The good agreement between theory and experiment in Table 2 shows that the present theory is an adequate description of the effect of extinction to the level at which the integrated intensity is reduced by a factor of 2. Data over a range of wavelengths and scattering angles will be collected at the intense pulsed source to provide a more stringent test.

8. Conclusions

First, it has been demonstrated that primary extinction within individual grains can have a marked effect on the result of a powder experiment. The absolute value of the temperature factors and their variation with temperature will be a function of grain size. Secondly, an expression for the extinction parameter suitable for inclusion in a Rietveld-type analysis is

$$y = (1+x)^{-\frac{1}{2}}, \qquad x = \left(\tfrac{3}{4} N_c F \lambda D\right)^2.$$

In the expression for the calculated intensity, each ordinate of the Bragg peak should be multiplied by y. Extinction does not affect the level of diffuse scattering in crystals of the size considered in this work, since the differential scattering cross section for incoherent (resulting from disordered nuclei or nuclear spin states) or coherent (thermal) diffuse scattering is very much lower than the differential cross section for Bragg scattering.

The natural parameter in a refinement is the grain diameter D; however, the resultant numerical value should be consistent with the grain, or subgrain, size found by electron microscopy.

Acknowledgments

I am indebted to Dr J. D. Jorgensen and Dr J. Faber, Jr for stimulating discussions on the analysis of powder data from pulsed sources, during a period I spent at the Argonne National Laboratory with the support of the U.S. Department of Energy. I thank Dr R. L. Davies for obtaining the neutron powder patterns, Ms Joanne Hodge for her work on specimen preparation, and Mr W. Kalceff for computing assistance.

References

Barron, T. H. K. (1977). *Acta Crystallogr.* A **33**, 602–4.
Becker, P. J., and Coppens, P. (1974). *Acta Crystallogr.* A **30**, 129–47.
Beg, M. M. (1976). *Acta Crystallogr.* A **32**, 154–6.
Cassels, J. M. (1950). *Prog. Nucl. Phys.* **1**, 182–215.
Ekstein, H. (1951). *Phys. Rev.* **83**, 721–9.
Fermi, E., Sturm, W. J., and Sachs, R. G. (1947). *Phys. Rev.* **71**, 589–94.
Hamilton, W. C. (1957). *Acta Crystallogr.* **10**, 620–34.
Hewat, A. W. (1974). Profile refinement of neutron powder diffraction patterns: Crystal and magnetic structures. Institüt Laue–Langevin Rep. No. 74 H625.
Howard, C. J., and Sabine, T. M. (1974). *J. Phys.* C **1**, 3454–65.
Marshall, W., and Lovesey, S. W. (1971). 'Theory of Neutron Scattering', p. 28 (Clarendon: Oxford).
Michell, J. W., and Belz, M. H. (1950). 'The Elements of Mathematical Analysis', p. 619 (Macmillan: London).
Rietveld, H. M. (1969). *J. Appl. Crystallogr.* **2**, 65–71.
Sabine, T. M. (1980). *Aust. J. Phys.* **33**, 565–72.
Sabine, T. M., and Clarke, P. J. (1977). *J. Appl. Crystallogr.* **10**, 277–80.
Sabine, T. M., and Dawson, B. (1963). Int. Conf. on Beryllium Oxide, Paper 34 (Australian Atomic Energy Commission: Sydney).
Sanger, P. L. (1969). *Acta Crystallogr.* A **25**, 694–701.
Whitaker, M. D., and Bayer, H. G. (1939). *Phys. Rev.* **55**, 1101.
Whittaker, E. T., and Watson, G. N. (1952). 'Modern Analysis', p. 123 (Cambridge Univ. Press).
Wilkins, S. W. (1980). *Phil. Trans. R. Soc. London* **299**, 277–312.
Wilson, A. J. C. (1949). 'X-ray Optics' (Methuen: London).
Zachariasen, W. H. (1945). 'Theory of X-ray Diffraction in Crystals' (Wiley: New York).
Zachariasen, W. H. (1967). *Acta Crystallogr.* **23**, 558–64.

Manuscript received 19 November 1984, accepted 1 May 1985